Permeability of Gigaporous Particles

James F. Pfeiffer, John C. Chen, and James T. Hsu
Dept. of Chemical Engineering, Lehigh University, Bethlehem, PA 18015

The volumetric flow rate of liquid and gas through small gigaporous particles was measured by a new method that isolates single particles in a test apparatus. To our knowledge, this is the first direct confirmation of flow through gigaporous particles made at pressure drops experienced during normal operation. High-performance liquid chromatography particles from 30 to 50 μm in diameter, previously reported to exhibit convection-enhanced intraparticle mass transfer, were studied. Using a CFD model of the test system, the permeability of individual particles was determined from the pressure-drop–flow-rate relationship. The average measured permeability of the particles studied is 7.89×10^{-15} m^2 with no dependence on particle size. This is 4 to 17 times greater than values calculated from models currently used to estimate the permeability of these kinds of particles. No other experimentally measured values of permeability have been reported for particles of this size. The results of this study might imply that the intraparticle structure does not behave like a bed of uniformly packed microspheres, but rather as an inhomogeneous assemblage of microparticles. The measured permeability values offer the possibility of developing better models of the intraparticle flow field under normal operating conditions. Knowledge of the intraparticle flow field is an important step in deriving predictive models of convective mass transfer in these types of particles.

Introduction

Many processes, such as heterogeneous catalysis, fermentation, and adsorptive separations, involve the transfer of chemical species from a mobile fluid phase onto the surface of a stationary solid phase. In most cases, the transfer involves diffusion of the species through a stagnant portion of the fluid, either inside the pores of a particle or across a stagnant boundary layer around a particle. The rate of mass transfer depends on the diffusion path length from the moving fluid to the active surface of the solid particle. The development of particles with interconnected pores, termed "gigapores," holds promise for enhancing mass-transfer rates by shortening the diffusion path length.

There are a number of strategies for improving mass-transfer rates including mounting the active material inside a membrane, using nonporous particles, and decreasing the size of porous particles. Each of these strategies has been employed, but each has disadvantages. Both membranes and nonporous particles decrease the surface area to volume ratio of the material, thereby decreasing the specific capacity. Using smaller particles increases the pressure drop required to move fluid through a packed bed composed of the particles. This is illustrated by recent developments in the supports used in high-performance liquid chromatography (HPLC). In the quest for faster separations, manufacturers have developed smaller particles, some as small as 3 μm in diameter, and nonporous particles that allow the user to operate at higher column flow rates. However, the disadvantages are higher pressure drops and lower column capacity, respectively. Indeed, there is little opportunity to further reduce the diameter of HPLC particles because the inlet pressures needed to operate the columns, which are on the order of 35 MPa, are near the operating limits of the equipment. In addition, columns containing smaller particles are more likely to clog. On the other hand, nonporous particles have insufficient capacity for commercial-scale separations. Thus, other approaches are needed to improve the speed of chromatographic separations that can be used on a preparative scale.

The more recent strategy proposed for increasing the speed of chromatographic systems uses 10- to 50-μm-dia. particles with large transecting pores connected to smaller pores that have larger specific areas (Afeyan et al., 1990). The large pores are intended to allow forced convective transport

Correspondence concerning this article should be addressed to J. C. Chen.

through the interior of the particles, thereby requiring diffusive transport in the smaller pores only. The larger particle size reduces the inlet operating pressures required to run the columns at high superficial bed velocities.

The concept that convection could enhance intraparticle mass transfer was first proposed by Wheeler (1951), although he concluded that it was only important in high-pressure gas systems using supports with very large pores. Later, Nir and Pismen (1977) used mathematical models to show that the mechanism could also be important in liquid systems. Experimental verification of the models was attempted by Cogan et al. (1982), who measured the apparent effect of forced convection on a catalytic reaction; the rate of depolymerization of paraldehyde on nickel sulfate supported on porous silica gel. They found that the effective reaction rate increased with increasing intensity of convective flux outside the porous pellets. Around the same time, Rodriguez et al. (1982) found that intraparticle forced convection could affect the calculation of effective diffusivities derived using unsteady-state techniques. In experiments using a hydrogen tracer in BM329 catalyst, they found a tenfold increase in apparent effective diffusivity as the packed-bed Reynolds number increased from 5 to 200. More recently, Dean et al. (1986) reported on the use of high-porosity (0.6 to 0.9) collagen beads with large pore diameters (10 to 50 μm) for immobilizing organisms in continuous mammalian cell fermentation. They suggested that the high porosity and large pore diameters allowed for intraparticle convection, which contributed to the overall rate of intraparticle mass transfer.

The possibility that this phenomenon could occur in chromatographic systems was first suggested by van Kreveld and van den Hoed (1977). They noted an apparent increase in mass-transfer rate with increasing superficial velocity in chromatography columns packed with Poracil C. In their experiments, the height of a theoretical plate (HETP) did not increase with increasing column bulk flow rate for molecules with low diffusivities as would be predicted by conventional theory. They attributed the improved mass transfer to eddies caused by the mobile phase flow, which extended into the pores of the particles. These eddies produced a flow-related increase in the effective intrapore diffusivity:

$$D_{r(\text{eff})} = D_r + \upsilon D_{\text{eddy}}, \tag{1}$$

where $D_{r(\text{eff})}$ is the effective diffusion coefficient inside the pores, D_r is the hindered diffusion coefficient inside the pores, υ is the linear velocity of the mobile phase in the column, and D_{eddy} is the coefficient of eddy diffusion.

Lloyd and Warner (1990) reported on the difference between the performance of PL-SAX 4,000 Å and PL-SAX 1,000 Å, the latter having smaller pores, in gradient elution chromatography. They found that with a short gradient development time the resolution factor increased significantly with increasing flow rate for the 4,000-Å material, but not the 1,000-Å material. They suggested that this was due to a difference in the intraparticle mass transfer of the two materials for large molecules because there was a decrease in the peak width with the large pore matrix, but not the small pore matrix. Plate count measurements from an isocratic system packed with the 4,000-Å particles showed that above a critical linear velocity, the efficiency improved irrespective of solute size, suggesting an apparent increase in the diffusion coefficient. As the authors point out, this is "not typical for porous materials." Afeyan et al. (1990, 1991a,b) proposed that the cause of this phenomenon was convective enhanced intraparticle mass transfer and described it as "perfusive chromatography." The advantages were an apparent reduction of the resistance to mobile-phase mass transfer without sacrificing high adsorbent capacity or necessitating extremely high-pressure operation. The system provided reduced retention times for high molecular weight molecules without loss of resolution. The effect was apparently accomplished by the flow of liquid through large "macropores" (or gigapores), which are on the order of 400–800 nm in diameter and which transect the particle. Electron photomicrographs of the particles, along with data from frontal analysis and observed column efficiency, suggest that fluid may indeed be flowing through the gigapores. However, the authors point out: "experimental confirmation of (flow through the particles) is difficult. Experimental techniques that test liquid flow through a...porous particle have not been described." Thus, to date, the existence of flow within particles is still a matter of conjecture based only on indirect evidence.

Directly demonstrating the existence of intraparticle flow is difficult for several reasons. First, the fraction of the total flow through a packed bed that goes through the particles at any point in the bed is very small. Afeyan et al. (1990) estimate it at less than 2%, Carta et al. (1992) place the range at 0.1 to 5%, depending on the permeability of the particles. This makes interpolation of the intraparticle flow from bulk flow rates through the bed impractical. Second, the magnitude of the flow rate through a single particle under normal operating conditions is small. Calculation using Darcy's law of the volumetric flow of water through a single 50-μm-diameter particle with permeability in the range that the manufacturer of the HPLC particles suggests gives a rate of around 10^{-12} to 10^{-13} m^3/s. Finally, the pressure drop across a single particle, even in high-pressure systems such as HPLC, is only on the order of 100–4,000 Pa. Therefore, to determine the existence of intraparticle flow and measure it with sufficient accuracy to allow for determination of the particle permeability requires an experimental technique that can isolate the flow through a single particle; generate a stable pressure drop across the particle in the desired range; and provide quantitative measurements of very low volumetric flow rates. Ideally, the technique should have the ability to measure the flow of both liquids and gases since gigaporous particles can be used in both types of systems. Finally, the experimental measurements must allow for determination of the particle permeability in order to extend the results to other systems containing these particles.

Our objective was to determine if intraparticle flow can occur under conditions similar to those in a chromatography column and then to use the relationship between intraparticle convection and pressure drop to estimate Darcy's constant (permeability) of the test particles. Comparison between the particle permeability determined from experimental measurements and those calculated by other investigators using various models can provide insight into the usefulness of the models in estimating the permeability of these types of particles. Permeability can also be used to model the intraparticle flow field in any pressure field that the particle might

experience, such as in a packed bed. Once the intraparticle flow field is known, it can then be used to develop first-principle models of the intraparticle mass transfer.

Experiment

To investigate this phenomenon, we developed a method of immobilizing individual particles in a test cell that seals the outer circumference and prevents flow around the outside of the particle. All of the flow through the cell must pass through the particle. We measure the flow using a device that we developed that generates a constant pressure drop of between 300 and 1,300 Pa and that can measure water flow rates as low as 10^{-14} m^3/s and gas flow rates as low as 10^{-12} m^3/s. This covers the range of operating conditions used in systems that contain these materials and the range of expected flow rates for commercially available perfusive HPLC supports in the 10–50-μm-dia. range. This test method does not create the same pressure field as that in a packed bed. However, the magnitude of the pressure drop across the individual particle is similar to that in packed beds under normal operating conditions. The apparatus can be used to measure the flow rate of either liquids or gases.

The experimental apparatus, shown in Figure 1, consists of two parts: a test cell and the low-volume flow-measuring (LVFM) device. Each test cell is composed of a piece of precision polyimide-coated fused silica tubing, 30, 40 or 50 μm (Polymicro Technologies, Phoenix, AZ), "potted" into a piece of stainless steel tubing that has a Swagelok connector on one end. The flow-measuring device consists of a precision site glass held at both ends by fluid-tight fittings. The ID of the site glass varies less than 0.013 mm over its entire length. The upper end of the side glass is open to the atmosphere and a test cell is attached to the lower end by a fluid-tight swaged connector. Twice-filtered, degassed, purified water is used for these tests. An additional 0.22-μm filter is placed between the site glass and the test cell for liquid flow measurements to prevent debris from the test apparatus from clogging the test cell.

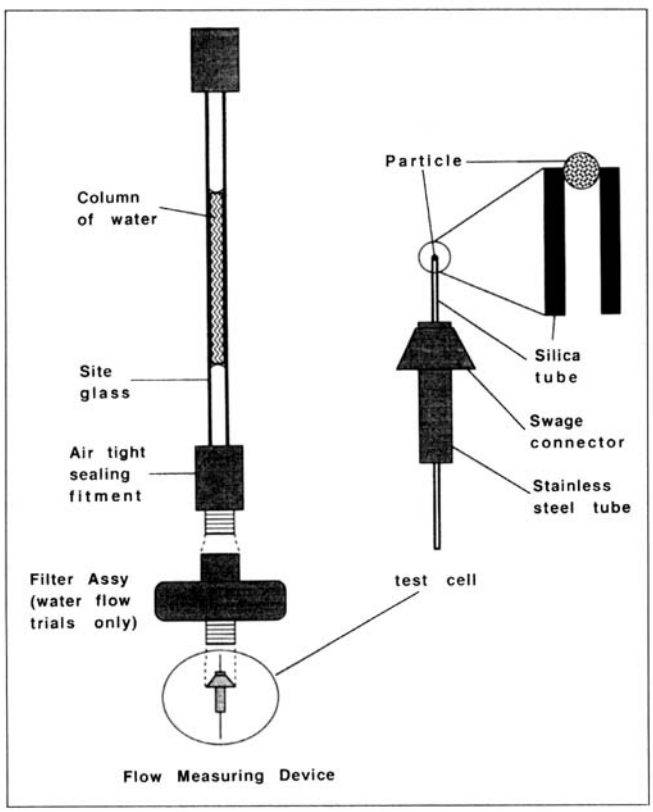

Figure 1. Low-volume flow-measurement apparatus and test cell.

For each trial, a single particle of slightly larger diameter than the silica tubing was placed in the entrance of the silica tube. The particle was sufficiently large to ensure a slight compression fit between the particle and the tube wall to prevent fluid from flowing around the outside of the particle. The test cell was then attached to the flow-measuring device and a column of water was placed near the bottom of the site glass. The column of water served two purposes; to generate the upstream pressure in the LVFM, and to measure the volumetric flow rate through the test cell. Since both the inlet of the site glass and the outlet of the test cell were open to the atmosphere, the pressure drop across the test cell equaled the hydrostatic pressure at the bottom of the column of water. When measuring air flow, an air space was left between the water and the test cell. When measuring water flow, the water column extended all the way to the test cell. The filter assembly that held the 0.22-μm filter used in the water-flow trials added some additional length to the column of water, but did not add any measurable resistance to flow at the rates measured in these trials. The volumetric flow rate was determined by measuring the displacement of the column of water in the site glass over timed intervals of 3 to 25 min each. At least three displacement (flow rate) measurements were made at each test pressure drop for air flow and at least two for water flow. For each test cell, the flow rate was measured at a minimum of four pressure drops of between 400 and 1,250 Pa for air-flow trials and one to three pressure drops, depending on the size of the particle being tested, of between 2,000 and 4,700 Pa for water-flow trials. The particles selected for this series of tests were 50 μm nominal (25–67 μm) diameter HPLC supports (POROS-OH 50, PerSeptive Biosystems, Cambridge, MA) that have been reported to exhibit the flow-dependent mass-transfer effect. Before placing the particle, each test cell was calibrated by measuring the volumetric flow rate vs. pressure drop relationship. The internal radius of the silica tube was then calculated from the Hagen-Poiseuille relationship:

$$R_{\text{tube}} = \left[\frac{8Q\mu L}{\pi \Delta P}\right]^{1/4}. \qquad (2)$$

After mounting the particle in the silica tube, the fit was verified visually at 180× magnification to ensure that the particle was not damaged during placement and that there were no visible gaps between the particle and the tube wall. Electron photomicrographs were taken of selected test cells to verify the sealing method. In all cases, the system was allowed to come to thermal equilibrium with the surroundings for at least one hour before any flow rate measurements were made. The ambient temperature was measured continually during each trial to ensure that errors due to thermal expansion of the air in the apparatus were not introduced.

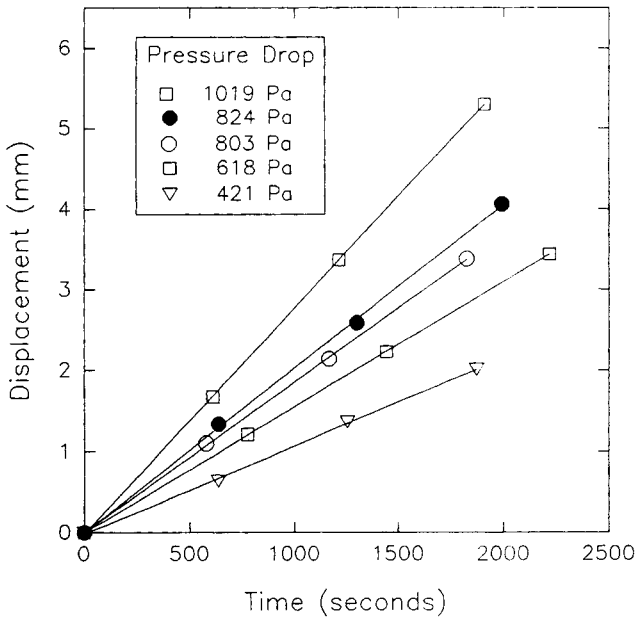

Figure 2. Displacement of water in the LVFM site glass over time for a single air-flow trial.

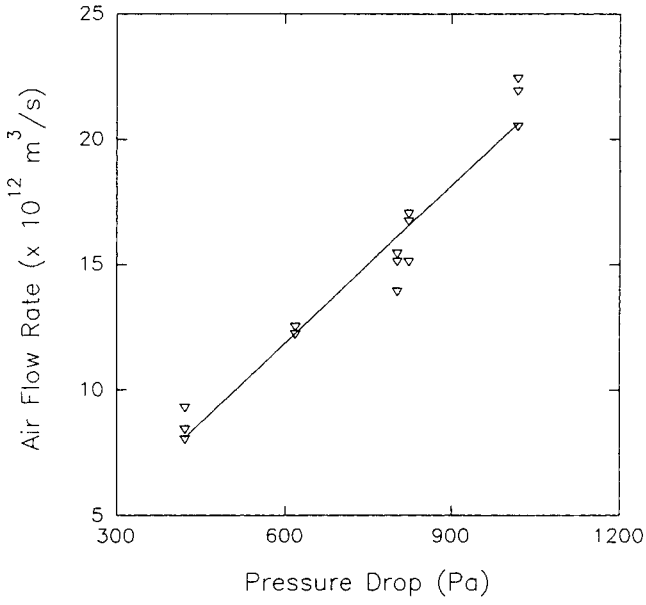

Figure 3. Measured volumetric air-flow rates at different pressure drops for a single trial.

Experimental Results

A total of 48 air-flow trials were conducted on particles of 30, 40 and 50 μm nominal diameter. Of these, 39 trials were conducted on the perfusive particles and 9 were conducted on nonperfusive particles of the same base material. Figure 2 shows the cumulative volume displaced vs. time for a typical air-flow trial of a test cell containing a 50-μm-dia. porous particle. The cumulative displacement increased linearly with time, which means that the flow through the test cell is constant over time. In comparison, there was no measurable air flow through any of the 9 test cells that contained nonperfusive particles. There was some variability from measurement to measurement caused by small fluctuations in the temperature of the test apparatus and errors in the displacement measurements. The displacement/time measurements were converted to volumetric flow rates using the cross-sectional area of the glass tube in the LVFM. The air-flow-rate measurements varied less than $\pm 10\%$ at any pressure drop and were on the order of 5 to 30 $\times$ 10^{-12} m^3/s. Figure 3 shows the volumetric flow rate vs. pressure-drop relationship for the same test cell. The volumetric flow rate through the test cell with the particle in place was about 10% of that without the particle. Thus, the particle introduces a significant resistance to flow. Analysis of the results using linear regression analysis gave correlation coefficients > 0.94 for all trials, indicating that flow rate varies linearly with pressure drop.

After completing the air-flow measurements, the water-flow rate was determined for nine test cells containing porous particles. The water-flow trials included test cells of all three sizes. The cumulative displacement increased linearly with time as shown in Figure 4 for a single trial. The displacement/time measurements were converted to volumetric flow rates as described earlier. The water-flow rate remained consistent for only a few hours, after which it decreased, apparently because the particle began to clog. This can be seen at the 3,648-Pa pressure drop that was the last of this trial. Note that the second point is lower than would be predicted by extrapolation of the first point. Therefore, only measurements made before the rate declined were used to evaluate the particle. In some trials the flow rate remained constant only long enough to make measurements at a single pressure drop. In those cells where the water-flow rate could be measured at more than one pressure drop, the relationship was linear between flow rate and pressure drop, as shown in Figure 5. The water-flow rates were lower than those for air, on the order of 0.4 to 2.5 $\times$ 10^{-12} m^3/s, despite the higher test

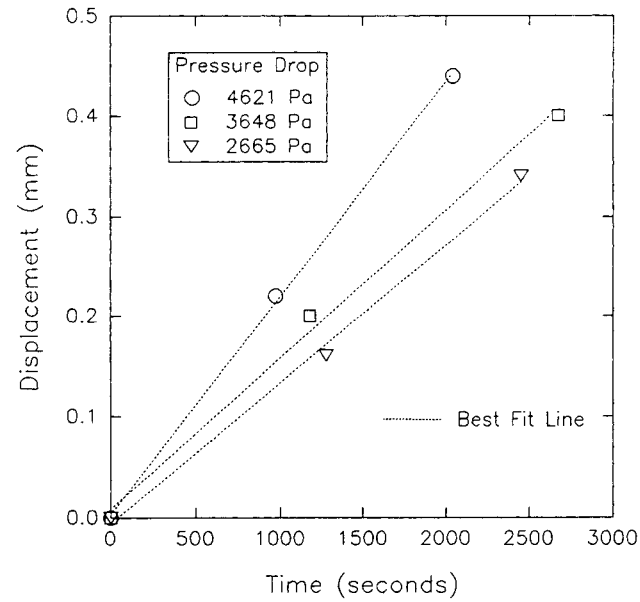

Figure 4. Displacement of water in the LVFM site glass over time for a single water-flow trial.

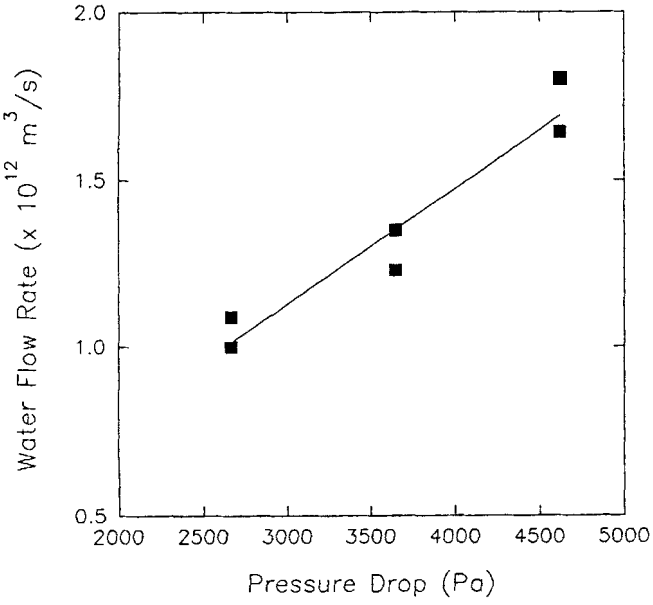

Figure 5. Measured volumetric water-flow rates at different pressure drops for a single trial.

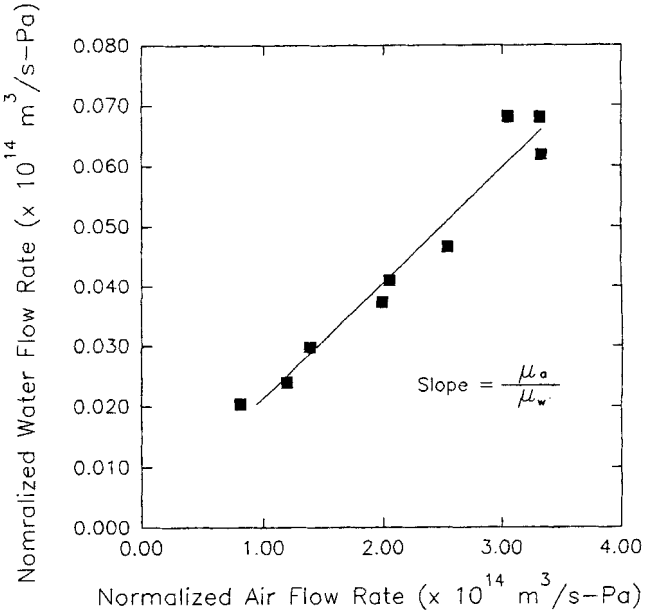

Figure 6. Comparison of air- and water-flow rates for 50-μm-dia. particles.

pressure drops used for the water-flow measurements. Figure 6 shows the relationship between normalized volumetric flow rate (flow rate/Pa pressure drop) of air and water through particles of all three sizes. The slope of the best fit regression line shown on the figure is 0.0200, which is within 2% of the ratio of the viscosity of air to the viscosity of water at the test conditions (0.0204). This suggests that the particles have the same permeability to air and water. The permeability can be determined from the flow-rate–pressure-drop measurements using a suitable model of the flow through the test system.

Determination of Particle Permeability

The intraparticle flow through a permeable particle can be described by Darcy's law:

$$v_p = -\frac{K}{\mu}\nabla P \tag{3}$$

where v_p is the intraparticle fluid velocity, K is the particle permeability, μ is the fluid viscosity, and ∇P is the pressure gradient inside the particle. However, the geometry of the test cell does not allow the flow through the particle to be modeled analytically. Therefore, a computational fluid dynamics (CFD) model of the particle and the test cell was constructed using Flow3D (AEA-CFDS, Pittsburgh, PA), a commercial CFD package capable of modeling porous media. The geometry of the model consisted of the first 150 μm of silica tubing with the particle at the upstream entrance. We did not include the remaining length of the tube because the flow in that portion is steady laminar ($Re < 10$). The particle was represented as an isotropically permeable sphere with flat areas at the equator equal to 4% of the particle diameter where the particle sealed against the tube. These flat areas were introduced to prevent a singularity in the pressure gradient that would occur if point contact between the particle and tube was used. Examination of the seal area by light and electron microscopy indicates that the seal has a finite length. This is due to small irregularities in the surface of the particle that are on the order of several microns in length. These irregularities are sheared off or compressed during mounting of the particle, leaving a small flat area at the seal. Electron photomicrographs of the surface of the particle show that the irregularities are on the order of 1 to 2 μm in size. The boundary conditions in the model were a constant pressure on the upstream face of the particle (representing the fluid reservoir conditions inside the LVFM) and a lower constant pressure on the radial plane of the tube (representing the beginning of the portion of the tube that has fully developed laminar flow). The pressure drop in the length of silica tubing not included in the model was determined analytically from the Hagen–Poiseuille relationship. The commercial package uses a modified Brinkman equation (1947) to model flow through porous media:

$$\nabla P = -\frac{\mu}{K}v + \mu'\nabla^2 v, \tag{4}$$

which combines Darcy's law with the viscous terms of the Navier–Stokes equation. In this equation, μ and μ' are the viscosity of the fluid outside and inside the porous media, respectively. In the case of laminar flow through the porous media, μ and μ' have been demonstrated experimentally to be the same (Neale et al., 1973). In the limit of $K/R_p^2 \ll 1$, the equation reduces to Darcy's law. Appropriate pressure and/or velocity boundary conditions must be specified for the specific geometry of the flow. Pressure boundary conditions were used in this model, as noted earlier. The overall volumetric air-flow rate through the model was determined by numerically integrating the velocity profile over the entire outlet of the tube using a Fortran subroutine provided by AEA-CFDS. In addition, a graphical depiction of the velocity

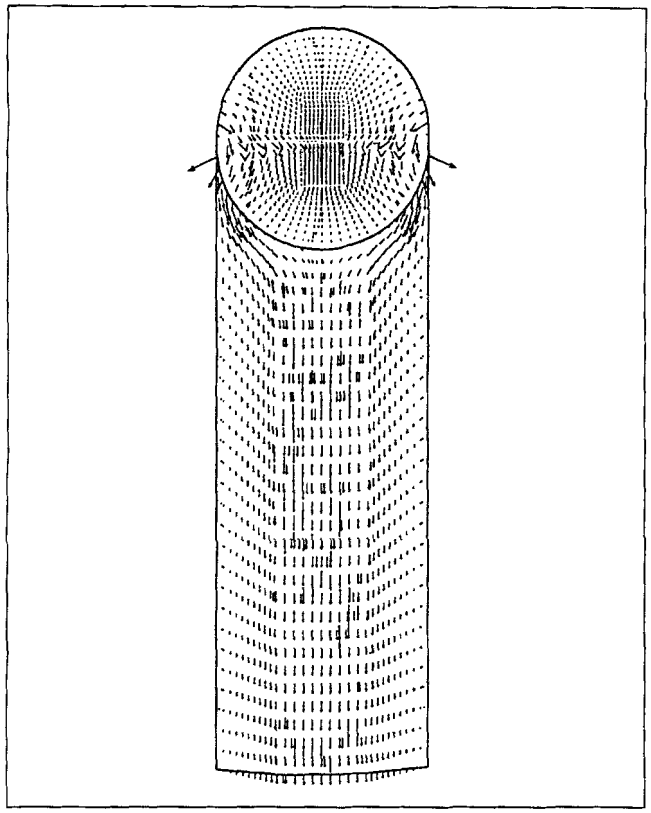

Figure 7. CFD model of velocity profiles through a uniformly permeable particle mounted in a tube.

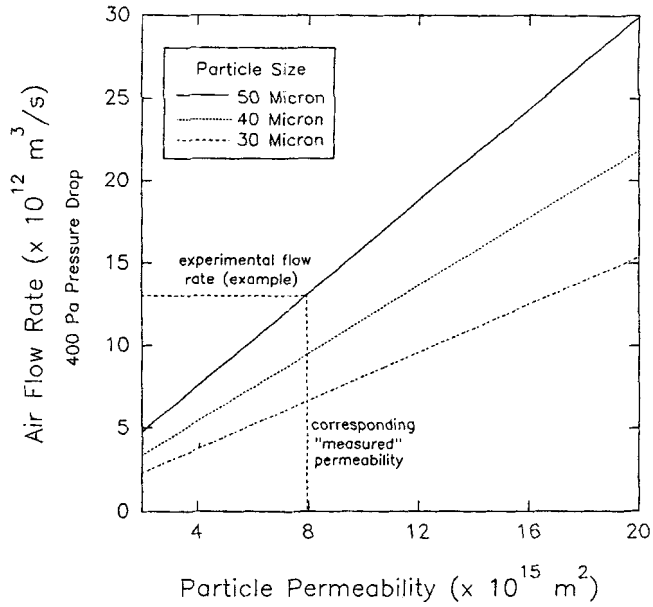

Figure 8. Volumetric air-flow rates as a function of particle permeability for three particle diameters as determined by the CFD model.

Measured permeability of a test particle is determined by matching the experimental air-flow rate to that calculated by the CFD model and then finding the corresponding permeability on the figure.

field in the model, shown in Figure 7, was used to verify the assumption that the velocity profile at the outlet of the tube was parabolic and therefore consistent with the Hagen–Poiseuille equation. The flow pattern in the model was the same for air and water, as would be expected, since both behave as noncompressible Newtonian fluids under the test conditions. Note that the actual velocity at any point in the interior of a test particle would not necessarily be the same as that shown by the model because the model represents the particle as a group of cells all having the same permeability. The particle itself has void areas and solid areas with flow occurring only in the voids. The model does not attempt to recreate the exact internal structure of the particle; however, the model should accurately predict the total volumetric flow rate through a particle of the permeability specified in the model.

Each run of the model was allowed to continue until the residual error in the mass flow rate through the outlet of the tube was less than 1%. The volumetric flow rate was calculated at four different permeabilities for each of the three particle sizes. In addition, the flow rate was calculated for a single particle size and permeability at four pressure drops to verify the expected linearity of the relationship. A plot of volumetric flow rate vs. permeability for a pressure drop of 400 Pa is shown in Figure 8 for the three nominal particle sizes. The relationships are linear ($R^2 > 0.999$) over the range of permeabilities that were calculated (6.2 to 18.6 $\times$ 10^{-15} m^2). This covers the corresponding range of flow rates measured experimentally during the trials. To determine the sensitivity of the model to the length of the seal area, geometric representations of the particle in the flow cell were constructed with flat areas of 4% and 8% of the nominal particle diameter. Doubling the seal length caused only a 12–14% decrease in flow rate through the model test cell. Therefore, the model appears to be fairly insensitive to this parameter. Models using a seal length of 4%, corresponding to 1.2 and 2.0 μm (depending on the nominal particle diameter), were used to determine the particle permeability because they were most consistent with estimates of the seal length based on electron photomicroscopy.

The permeability of the test particles was determined from the CFD model using both air and water flow rate measurements for all three particle sizes. The permeability to air of each test particle was derived from the numerical model described earlier. The results are shown by particle size in Figure 9. The overall average permeability was 7.89 $\times$ 10^{-15} m^2 with no dependence on particle size as determined by analysis of variance. Since HPLC systems often use aqueous or other Newtonian fluid solvent systems, the permeability of the test particles to air was compared to that of water for nine particles (three of each size). These are shown in Table 1. Note that the average air permeability is very close to that of water for all particle sizes.

Correlations and Models of Permeability

The first step in developing models of convective enhanced mass transfer is to determine the intraparticle flow field. Rodrigues et al. (1982) developed a model for systems of simultaneous convection and reaction in a slab geometry. They proposed an enhancement factor of the diffusivity of a species that is given by:

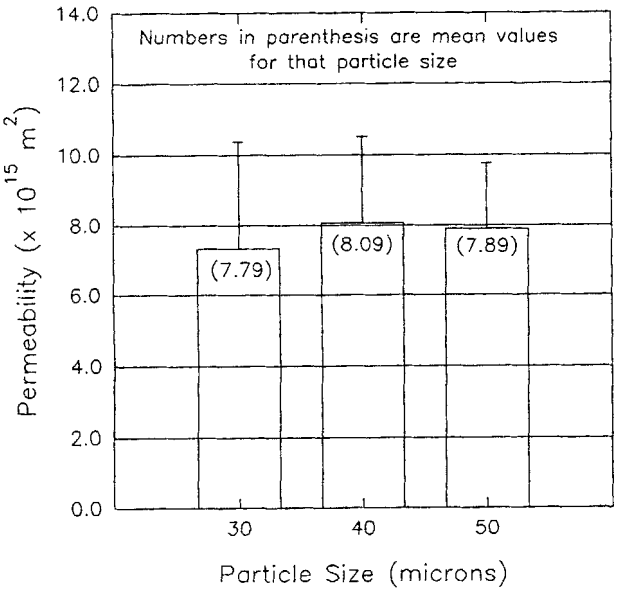

Figure 9. Air permeability of POROS 50 HPLC particles by particle diameter.

Large bars indicate mean permeability for that particle size. Error bars, shown in positive direction only, are one standard deviation.

$$D_{\text{eff}} = \frac{D}{f(\lambda)}$$

where

$$f(\lambda) = \frac{3}{\lambda}\left(\frac{1}{\tanh \lambda} - \frac{1}{\lambda}\right), \tag{5}$$

where λ is the intraparticle Peclet number: $v_p d_p/2D$. A similar model is proposed by Afeyan et al. (1990), in which the enhancement in intraparticle effective diffusivity is proportional to the intraparticle fluid velocity. As discussed previously, the intraparticle fluid velocity is a function of the permeability of the porous particles. Carta et al. (1992) calculated that the ratio of the intraparticle fluid velocity to the superficial bed velocity varies from 0.1% to 5% as the permeability of the particle increases from 10^{-16} to 10^{-15} m^2. Thus, a small change in the particle permeability can have a significant effect on the intraparticle fluid velocity. In the models presented to date, the particle permeability is derived from the Carmen–Kozeny equation:

$$K = \frac{\epsilon^3 d_m^2}{150(1-\epsilon)^2}, \tag{6}$$

Table 1. Permeability to Air and Water of Perfusive HPLC Particles of Three Diameters

Particle Dia. μm	No.of Trials	Air Permeab. 10^{-15} m^2	Water Permeab. 10^{-15} m^2
30	3	6.63	7.50
40	3	9.79	9.84
50	3	7.63	7.57

where ϵ is the particle void fraction, and d_m is the diameter of microspheres that make up the particle. This equation is most accurate for materials that behave as well-packed beds of uniformly sized particles. Afeyan et al. (1990) suggest substituting the gigapore diameter adjusted for the tortuosity of the fluid path [$d_m = r(d_{\text{pore}})$, r being tortuosity] for the microsphere diameter in the Carmen–Kozeny equation. To examine these estimates, we compared the porosity calculated using each of the two methods to that obtained experimentally. Electron microscopy of the particles showed that the microspheres are relatively nonporous, and therefore we estimated their diameter from the geometric relationship:

$$\left(\frac{\text{Surface area}}{\text{Volume}}\right)_{\text{sphere}} = \frac{6}{d_{\text{sphere}}}, \tag{7}$$

where the surface-area-to-volume ratio was measured using Brunauer-Emmett-Teller analysis. The void fraction of the particles was estimated visually at 0.5. Adjusting the measured specific area of 15.43 m^2/g by the density of the material of the particles (1,050 kg/m^3), gives 3.70×10^{-7} m as the diameter of the microspheres and a corresponding permeability of 4.6×10^{-16} m^2. Reducing the specific area by one-third to account for small pore structures not visible under electron microscopy, as suggested by Lloyd and Warner (1990), gives an estimated permeability of 1.0×10^{-15} m^2. Calculation of the particle permeability by the method of Afeyan et al. (1990) using values of tortuosity and range of gigapore diameters published by the manufacturer gives permeability estimates of 0.53 to 2.1×10^{-15} m^2. As shown in Table 2, the measured values of the permeability are 8 to 17 times greater than the estimates using the Carmen–Kozeny equation, and 4 to 15 times greater than the estimates using the method described by Afeyan. This seems to indicate that these gigaporous particles do not behave as uniformly packed beds, and therefore it may not be appropriate to model them using either form of the Carmen–Kozeny equation. Electron photomicrographs of the particles show an isotropic internal structure but a nonuniform distribution of void spaces between the solid microspheres. From the measured permeability values, the particle appears to behave more like an inhomogeneous packed bed of microparticles with interstitial channels that carry much of the flow rather than a uniformly packed bed.

Table 2. Permeability: Measured vs. Calculated Using Variations of the Carmen–Kozeny Equation ($\epsilon = 0.5$ for All Calculations)

Measured Permeability	Carmen–Kozeny Equation	Afeyan Equation ($r = 2$)
$K = 7.89 \times 10^{-15}$ m^2	$d_m = 3.7 \times 10^{-7}$ m $\quad K = 0.46 \times 10^{-15}$ m^2	$d_{\text{pore}} = 200$ nm $\quad K = 0.53 \times 10^{-15}$ m^2
	$d_m = 5.6 \times 10^{-7}$ m $\quad K = 1.03 \times 10^{-15}$ m^2	$d_{\text{pore}} = 400$ nm $\quad K = 2.10 \times 10^{-15}$ m^2

Summary and Conclusions

Experimental measurement of the permeability of gigaporous particles using a new method that isolates the particle flow through individual particles gives values that are 4 to 17 times greater than those calculated using variations of the Carmen–Kozeny equation. Given the strong relationship between intraparticle velocity and permeability described by Carta et al. (1992), using the latter values of permeability may introduce substantial errors into estimates of the intraparticle velocity. Using measured values of the permeability of the particles should provide better estimates of the intraparticle flow field in various systems, including packed beds. This should allow for a better understanding of the magnitude of the enhancement in mass-transfer rates caused by intraparticle convection.

Acknowledgment

The authors gratefully acknowledge the financial support of the National Science Foundation (grant CTS-9311457) for this work and the U.S. Department of Education Fellowship (1991 to 1993) and Lehigh University Byllesby Fellowship (1993 to 1995) support for J. F. Pfeiffer. We are also grateful to Princeton Labs, Inc., Perkasie, PA, for their assistance in designing and constructing the flow-measuring apparatus used in these experiments.

Notation

D = diffusivity
d_p = particle diameter
d_{pore} = micropore diameter
L = length
Q = volumetric flow rate
Re = Reynolds number
R_p = particle radius
v_p = linear velocity of a mobile phase in a gigaporous particle

Literature Cited

Afeyan, N. B., N. Gordon, I. Mazsaroff, L. Varady, S. Fulton, Y. Yang, and F. Regnier, "Flow-Through Particles for the High-Performance Liquid Chromatographic Separation of Biomolecules: Perfusion Chromatography," *J. Chromatog.*, **519**, 1 (1990).

Afeyan, N. B., S. P. Fulton, and F. E. Regnier, "High-Throughput Chromatography Using Perfusive Supports," *Liquid Chromatog.-Gas Chromatog.*, **9**, 824 (1991a).

Afeyan, N. B., S. P. Fulton, and, F. E. Regnier, "Perfusion Chromatography Packing Materials for Proteins and Peptides," *J. Chromatog.*, **544**, 267 (1991b).

Brinkman, H. C., "A Calculation of the Viscous Force Exerted by a Flowing Fluid on a Dense Swarm of Particles," *Appl. Sci. Res.*, **A1**, 27 (1947).

Carta, G., H. Massadi, M. Gregory, and D. J. Kirwan, "Chromatography with Permeable Supports: Theory and Comparison with Experiments," *Sep. Technol.*, **2**, 62 (1992).

Cogan, R., G. Pipko, and A. Nir, "Simultaneous Intraparticle Forced Convection, Diffusion and Reaction in a Porous Catalyst: III," *Chem. Eng. Sci.*, **37**, 147 (1982).

Dean, R. C., S. B. Karkare, P. G. Phillips, N. G. Ray, and P. W. Runstadlet, "Continuous Cell Culture with Fluidized Sponge Beads for Large Production of Medical Proteins," Tech. Memo. TM-184A, Verax Co., Lebanon, NH (1986).

Lloyd, L., and F. Warner, "Preparative HPLC on a Unique High-Speed Macroporous Resin," *J. Chromatog.*, **512**, 365 (1990).

Neale, G., N. Epstein, and W. Nader, "Creeping Flow Relative to a Permeable Sphere," *Chem. Eng. Sci.*, **28**, 202 (1973).

Nir, A., and L. Pismen, "Simultaneous Intraparticle Forced Convection, Diffusion and Reaction in a Porous Catalyst: I," *Chem. Eng. Sci.*, **32**, 35 (1977).

Rodrigues, A. E., B. Ahn, and A. Zoulalian, "Intraparticle Forced Convection Effect in Catalyst Diffusivity Measurements and Reactor Design," *AIChE J.*, **28**, 541 (1982).

van Kreveld, M. E., and N. van den Hoed, "Mass Transfer Phenomena in Gel Permeation Chromatography," *J. Chromatog.*, **149**, 71 (1978).

Wheeler, A., "Reaction Rates and Selectivity in Catalyst Pores," *Adv. Catal.*, **3**, 250 (1951).

Manuscript received Mar. 2, 1995, and revision received May 24, 1995.